

# Electrostatics Favor PNA:DNA Stability over Stereochemistry in Pyrrolidine-Based Cationic Dual-Backbone PNA Analogues

Ashwani Sharma,<sup>\*,[a, b]</sup> Shahaji H. More,<sup>[a]</sup> and Krishna N. Ganesh<sup>[a]</sup>

Modifications to the peptide nucleic acid (PNA) backbone has been well known to alter the thermodynamical parameters of PNA:DNA complexes to broaden their utility for different applications. Electrostatic interactions between a modified PNA having a positively charged backbone and the negatively charged DNA has been shown to enhance thermal stabilities of PNA:DNA complexes at various instances. On the other hand, chiral introduction in PNA backbone leads to stereochemical preference that affects binding properties. However, the interplay between electrostatics and stereochemistry has not been systematically studied so far. Herein, we report the synthesis

and biophysical characterization of cationic PNA named *dap*PNA, first of its kind, having a dual PNA backbone constituting of a pyrrolidine ring having a  $\beta$ -substitution. One of the aims of this study was to investigate the role of electrostatics over stereochemical preferences. The results show that electrostatic attraction between cationic *dap*PNA and negatively charged DNA overcomes the unfavorable stereochemical effects and enhances stability of PNA:DNA complexes. Moreover, two different PNA backbones derived from a single PNA monomer expands the repertoire of pyrrolidine based PNA analogues.

## Introduction

Peptide nucleic acids (PNAs) are a class of designed synthetic molecules, which have emerged as one of the potential and effective analogues of DNA.<sup>[1,2]</sup> In PNA, the negatively charged sugar-phosphate backbone of DNA is replaced with a neutral and achiral polyamide backbone consisting of repeating *N*-(2-aminoethyl)-glycine (*aeg*) units, wherein the nucleobases are flanked through an acetyl linker.<sup>[3,4]</sup> PNA interacts with complementary DNA through sequence specific Watson-Crick base-pairing and being neutral without the anionic charges as in DNA, the PNA:DNA complexes are thermally more stable than the corresponding DNA:DNA complexes.<sup>[4-6]</sup> PNA is not a natural substrate for cellular enzymes and is thus resistant to both nucleases and proteases. In spite of superior molecular recognition properties towards DNA, the flexible and achiral backbone of PNA renders ambiguity in its binding orientation with DNA which can be both parallel (N–5') and antiparallel (N–3').<sup>[7]</sup> Further, inefficient cell uptake and poor aqueous solubility due to its non-ionic nature has limited its application as an antisense drug.<sup>[8,9]</sup> In order to overcome these limitations and tune the backbone conformation, several chemical modifications of PNA have been employed by introducing substituents on backbone

and side chains imparting chirality, making them cyclic, adding charges to enhance aqueous solubility and conjugating with ligands to target them to specific cells.<sup>[7,10-15]</sup> Various five/six membered carbocyclic and heterocyclic rings (Figure 1) preorganize the PNA backbone with conformational constrain for preferential DNA/RNA and parallel/antiparallel binding. The resulting chiral and charged PNA backbones are good probes to delineate the electrostatic and stereochemical effects on formation of PNA:DNA complexes.<sup>[7,16]</sup>

Electrostatic plays an important role in stabilizing the PNA:DNA complexes.<sup>[4]</sup> Extensive work on PNA modifications has shown that cationic PNAs increase the stability of PNA:DNA complexes due to electrostatic attraction of the positively charged PNA with the anionic phosphate backbone of DNA.<sup>[23-25]</sup> Creation of positively charged PNAs is achieved by anchoring amines or guanidine groups on side chains and by conjugating lysines at N/C-terminus that are protonated at physiological pH, making PNA backbone cationic. The stereochemistry of substituents at the C2–C3 position on the backbone affects the stability and imparts preferential binding of PNA to DNA (Figure 1). Nielsen *et al.*<sup>[17]</sup> reported *trans* cyclohexyl PNA (*trans-ch*PNA) in which the C2–C3 bond of ethylenediamine segment of PNA backbone is fused with cyclohexane ring in *trans* configuration of the substituents (Figure 1b). The (*S,S*) *trans* analogue showed binding similar to unsubstituted *aeg*PNA while the *trans*-(*R,R*) showed weaker binding with DNA. On the other hand, both the *cis-ch*PNA analogues (*R,S*) and (*S,R*) showed preferential binding with RNA compared to DNA with higher stability.<sup>[18]</sup> A similar phenomenon was observed for cyclopentyl PNA (Figure 1c), where the *trans*-(*S,S*)-*cp*PNA showed good thermal stability with DNA while the PNA with opposite stereochemistry *trans*-(*R,R*) does not bind to DNA.<sup>[19]</sup> In comparison, both RNA duplexes from the *cis-cp*PNA with (*R,S*) and (*S,R*) stereochemistry reported by

[a] Prof. Dr. A. Sharma, Dr. S. H. More, Dr. K. N. Ganesh  
Department of Chemistry,  
Indian Institute of Science Education and Research (IISER)  
Tirupati 517507, India  
E-mail: a.sharma@iiseritirupati.ac.in

[b] Prof. Dr. A. Sharma  
Department of Biology,  
Indian Institute of Science Education and Research (IISER)  
Tirupati 517507, India

Supporting information for this article is available on the WWW under  
<https://doi.org/10.1002/ejoc.202001581>

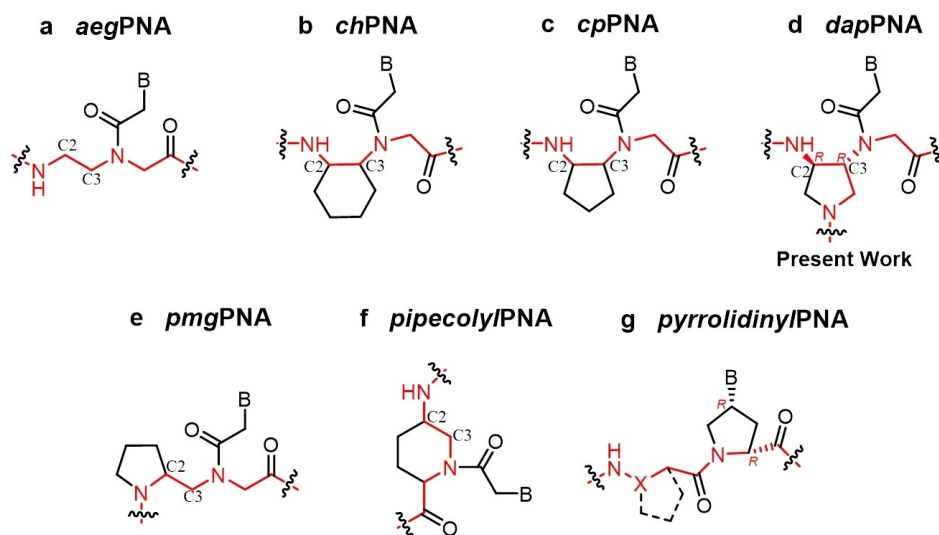


**Figure 1.** Chemical structures of different PNAs indicating C2–C3 carbons of PNA backbone, marked in red (a) Aminoethyl glycyl, *aegPNA*<sup>[1]</sup> (b) Cyclohexyl, *chPNA*<sup>[17,18]</sup> (c) Cyclopentyl, *cpPNA*<sup>[19,20]</sup> (d) Diaminopyrrolidine, *dapPNA* (e) N-(Pyrrolidinyl-2-methyl)glycine, *pmgPNA*<sup>[21]</sup>, (f) *pipecolylPNA*<sup>[22]</sup> and (g) *pyrrolidinylPNA*.<sup>[23]</sup>

Govindraju *et al.*<sup>[20]</sup> showed enhanced stability for both DNA and RNA hybrids. As discussed above, both *trans(R,R)* cyclohexyl and *(R,R)* cyclopentyl showed weaker or no binding to DNA which was attributed to their unfavorable stereochemistry.

To examine whether the introduction of electrostatic forces between the cationic PNA and negatively charged DNA can overcome unfavorable stereochemical effects in PNA/DNA binding, we hypothesized that insertion of a N atom in the cyclopentyl ring of *trans(R,R)*-*cpPNA* would make it cationic and thereby improve its binding to anionic DNA in addition to improving aqueous solubility of PNA. Such an introduction of N atom in cyclopentyl ring will also affect the 5-membered pyrrolidine ring puckering leading to better pre-organization of PNA backbone for favorable binding. Reports on Pyrrolidinyl based PNA having a modular dipeptide backbone by Vilaivan *et al* (Figure 1g) also suggests the importance of structural constraints over electrostatic interactions.<sup>[23]</sup>

Towards this goal, we designed *trans(R,R)*-3,4-diaminopyrrolidine based PNA monomer (*dapPNA*) in which the ethylenediamine unit of *aegPNA* is structural part of the pyrrolidine ring (Figure 1d). The orthogonally protected (Boc/Fmoc) *dapPNA* monomer (Figure 2A) can be employed in standard solid phase peptide synthesis (SPPS) through either Boc or Fmoc chemistry. Notably depending upon the direction of synthesis and choice of amino functionality at side chain, *dapPNA* monomer can give rise to two different PNA backbones from a single monomer unit. One PNA has backbone starting from a primary amine (Figure 2B), while the other PNA backbone initiated from a secondary cyclic amine (Figure 2C). Earlier attempts of using cyclic pyrrolidinyl amine in PNA backbone involved *N*-(pyrrolidinyl-2-methyl) glycine<sup>[21]</sup> (*pmgPNA*, Figure 1e) that binds to DNA weakly compared to the standard *aegPNA* and the weaker binding was attributed to lack of positive charge in the PNA backbone.<sup>[21]</sup> In the *secdapPNA* backbone (Figure 2C) is cationic due to protonated amine ( $\text{NH}_3^+$ ) in the pyrrolidine ring. Additionally, *dapPNA*

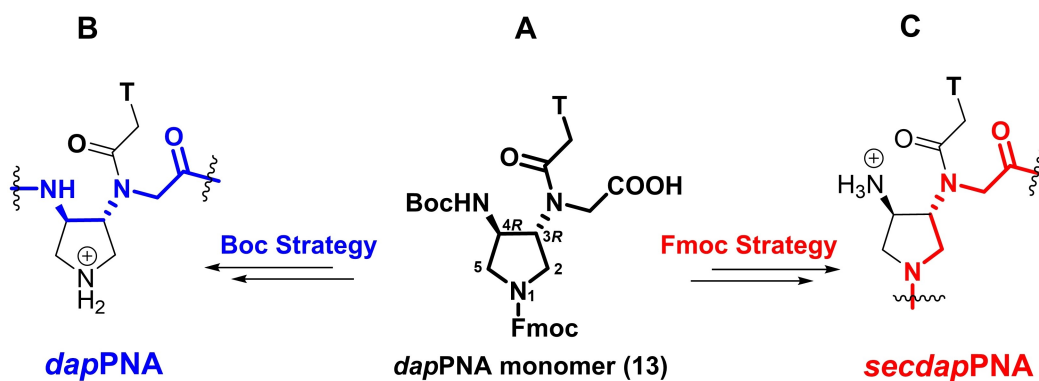


**Figure 2.** Chemical structures of (A) *dapPNA* monomer 13, (B) *dapPNA* and (C) *secdapPNA*.

constitutes a new class of PNA analogues having backbones derived from pyrrolidine ring having  $\beta$ -substitution instead of well-known  $\alpha$ -substituted pyrrolidines derived from proline.<sup>[21,23]</sup>

## Results and Discussion

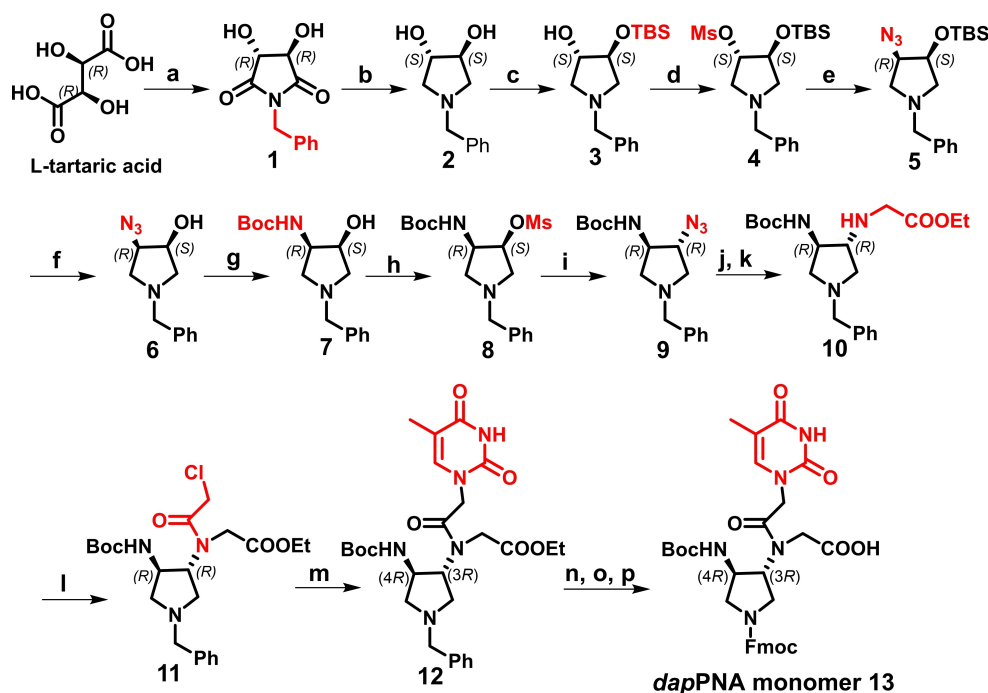
### Synthesis of (3R,4R)-Diaminopyrrolidinyl (dapPNA) Monomer 13

The synthesis of target monomer 13 (Scheme 1) was accomplished starting from the commercially available L-tartaric acid that was condensed with benzyl amine to obtain imide 1. Complete reduction of imide 1 was achieved using reducing agent LAH to get the diol 2 by slightly modifying the reported procedure.<sup>[26]</sup> The mono O-protection of diol 2 was attempted using *t*-butyldimethylsilyl chloride (TBDMS-Cl) in THF and using sodium hydride as base to yield compound 3 that was subjected to mesyl chloride to obtain O-mesylate 4. Compound 5 was obtained by  $S_N^2$  attack of azide ( $N_3^-$ ) to O-mesylate 4 with inversion of stereochemistry using sodium azide in dry DMF under heating conditions. The reaction also yielded azidoalcohol 6 as the minor product that was required for the next step. To obtain azidoalcohol 6 in good yield, compound 5 was O-desilylated to 6 using TBAF. The presence of azide group in both 5 and 6 was confirmed by IR. The azido alcohol 6 was reduced to amine selectively without N-benzyl removal using Raney-Ni and further *in situ* protected with Boc to obtain the compound 7.

Hydroxyl group in compound 7 was converted to O-mesyl derivative 8 followed by  $S_N^2$  inversion to give azide 9 in the presence of sodium azide under heating conditions. Compound 8 and 9 were obtained as crystalline solids and were characterized by single crystal X-ray diffraction. Azide 9 was further hydrogenated using Raney-Ni to obtain the corresponding amine, which was N-alkylated using ethyl bromoacetate to obtain 10. Acylation of 10 with chloroacetyl chloride provided compound 11 in good yield that was employed further for N1-alkylation of thymine using mild base  $K_2CO_3$  to yield ester 12. This ester was hydrolyzed with aq. sodium hydroxide gave the corresponding acid, which was subjected to *in situ* hydrogenation for N1-benzyl deprotection using Pd/C to obtain corresponding amine. This was protected with Fmoc chloride to obtain the desired dapPNA monomer 13 in overall good yield. The structural integrity of all the compounds was confirmed by  $^1H$ ,  $^{13}C$  NMR & DEPT spectroscopic analysis and mass spectrometry.

### Solid Phase Peptide Synthesis of PNA Oligomers

Peptide nucleic acids that have a pseudo peptide backbone can be synthesized by standard solid phase peptide synthesis (SPPS) using Boc/Fmoc strategy. dapPNA monomer 13 contains orthogonal protection with Boc and Fmoc groups and thus can be subjected to separate SPPS using either Boc or Fmoc chemistry giving rise to two different isomeric PNA backbones as shown in Figure 2. Assembly by Boc chemistry will build the dapPNA oligomer utilizing the primary amino function in the PNA



**Scheme 1.** a) Benzyl amine, Xylene, reflux, 6–7 h, (90%); b) LiAlH<sub>4</sub>, THF, reflux, 12 h, (73%); c) NaH, TBS-Cl, dry THF (80%); d) MsCl, Et<sub>3</sub>N, dry DCM, (75%); e) NaN<sub>3</sub>, DMF, 100 °C, 12 h, (48%); f) 1 M TBAF, dry THF, 2 h, (86%); g) H<sub>2</sub>, Raney-Ni, (Boc)<sub>2</sub>O, EtOAc, (74%); h) MsCl, Et<sub>3</sub>N, dry DCM, (83%); i) NaN<sub>3</sub>, dry DMF, 70 °C, 18 h, (86%); j) H<sub>2</sub>, Raney-Ni, EtOH; k) Ethyl bromoacetate, K<sub>2</sub>CO<sub>3</sub>, dry ACN, (71%); l) Chloroacetyl chloride, Et<sub>3</sub>N, dry DCM, (85%); m) Thymine, K<sub>2</sub>CO<sub>3</sub>, dry DMF, 18 h, (85%); n) 1 N aq. NaOH, EtOH; o) H<sub>2</sub>, Pd/C, EtOH:H<sub>2</sub>O (8:2), 18 h; p) Fmoc-Cl, NaHCO<sub>3</sub>, 12 h, (57%).

backbone while Fmoc chemistry provides *secdap*PNA oligomers that involves secondary amine of pyrrolidine ring in the PNA backbone.

The monomer **13** was incorporated at the desired sites within homo-oligomeric and the mixed *aeg*PNA sequences as *dap*PNA (represented by **t\***) using boc chemistry and as *secdap*PNA (represented by **t\***) using Fmoc chemistry during solid phase synthesis (Table 1). All PNA oligomers were purified by reverse phase HPLC and characterized by MALDI-TOF.

### Circular Dichroism (CD) Studies of PNA:DNA Complexes

To confirm the binding specificity and stoichiometry of PNA:DNA complexes, CD spectra for PNA oligomers, and their complexes

with cDNA were recorded. All single-stranded PNA oligomers exhibited very low induced CD signals (Figure S1, ESI). However upon binding with cDNA, all the PNA:DNA complexes showed strong CD signals corresponding to PNA<sub>2</sub>:DNA triplex for homopyrimidine PNAs (PNA1–PNA4) and PNA:DNA duplex for mixed sequences (PNA5–PNA8). A low intensity positive band at 258 and 285 nm (generally covering whole wavelength range 255–290 nm) along with moderate negative band at 250 nm characteristic of PNA:DNA:PNA triplex for homopyrimidine PNA (PNA1–PNA4) were observed (Figure 3A). However, mixed sequences (PNA5–PNA8), generally form PNA:DNA duplex and shows appearance of moderate positive band between 260–270 nm and a weaker negative band around 240 nm (Figure 3B). The modifications in control *aeg*PNA might alter base stacking patterns in their complexes with DNA leading to slight shift in

Table 1. HPLC Retention time, and MALDI-TOF characterization of PNA1–PNA14.

Entry no.	Sequence	Ret. time	Mol Formula	Cal. mass	Observed mass
PNA 1	TTTTTTTT-Lys	8.0	C <sub>94</sub> H <sub>127</sub> N <sub>35</sub> O <sub>33</sub>	2272.31	2275.70
PNA 2	<b>t*</b> TTTTTTTT-Lys	8.3	C <sub>96</sub> H <sub>130</sub> N <sub>36</sub> O <sub>33</sub>	2313.61	2314.32
PNA 3	TTT <b>t*</b> TTTT-Lys	7.8	C <sub>96</sub> H <sub>130</sub> N <sub>36</sub> O <sub>33</sub>	2313.61	2312.59
PNA 4	TTTTTTTT <b>t*</b> -Lys	8.0	C <sub>96</sub> H <sub>130</sub> N <sub>36</sub> O <sub>33</sub>	2313.61	2315.92
PNA 5	GTAGATCACT-Lys	7.9	C <sub>114</sub> H <sub>148</sub> N <sub>60</sub> O <sub>31</sub>	2852.52	2853.38
PNA 6	G <b>t*</b> AGATCACT-Lys	7.2	C <sub>116</sub> H <sub>151</sub> N <sub>61</sub> O <sub>31</sub>	2893.64	2916.46[M+Na]
PNA 7	GTAGAT <b>t*</b> CACT-Lys	7.0	C <sub>116</sub> H <sub>151</sub> N <sub>61</sub> O <sub>31</sub>	2893.64	2895.83
PNA 8	G <b>t*</b> AGAT <b>t*</b> CACT-Lys	7.0	C <sub>118</sub> H <sub>154</sub> N <sub>61</sub> O <sub>31</sub>	2934.73	2937.60
PNA9	TTACCTCAGT-Lys	7.5	C <sub>113</sub> H <sub>149</sub> N <sub>55</sub> O <sub>33</sub>	2804.18	2827.69[M+Na]
PNA10	T <b>t*</b> ACCT <b>t*</b> CAGT-Lys	7.6	C <sub>117</sub> H <sub>155</sub> N <sub>57</sub> O <sub>33</sub>	2886.27	2910.73[M+Na]
PNA 11	<b>t*</b> TTTTTTTT-Lys	8.2	C <sub>96</sub> H <sub>130</sub> N <sub>36</sub> O <sub>33</sub>	2313.61	2316.76
PNA 12	TTT <b>t*</b> TTTT-Lys	7.9	C <sub>96</sub> H <sub>130</sub> N <sub>36</sub> O <sub>33</sub>	2313.61	2316.66
PNA 13	TTTTTTTT <b>t*</b> -Lys	8.5	C <sub>96</sub> H <sub>130</sub> N <sub>36</sub> O <sub>33</sub>	2313.61	2316.08
PNA 14	G <b>t*</b> AGATCACT-Lys	7.6	C <sub>116</sub> H <sub>151</sub> N <sub>61</sub> O <sub>31</sub>	2893.64	2895.27[M+Na]

**t\*** = *dap*PNA and **t\*** = *secdap*PNA

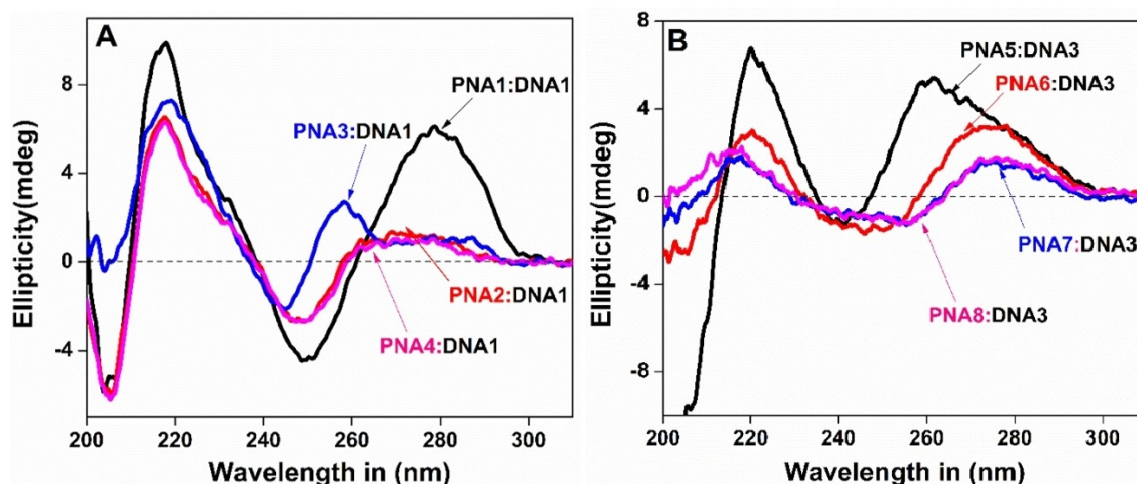


Figure 3. CD spectras (A) Triplexes of PNA1–PNA4 with complementary DNA1 (CGA<sub>8</sub>GC) (B) Duplexes of PNA5–PNA8 with antiparallel DNA 3 (AGTGATCTAC). Conditions: PNA concentration 2 μM in buffer, 10 mM sodium phosphate pH 7.4, 10 mM NaCl.

CD bands. PNA<sub>2</sub>:DNA triplex formation in case of homopyrimidine PNA3 was also confirmed by UV-Job's plot that confirms that homopyrimidine PNA3 bind to DNA1 in 2:1 stoichiometry (Figure S2, ESI).

### Thermal Stability of PNA<sub>2</sub>:DNA Triplex

The homo-oligomers of modified *dap*PNA1–4 were hybridized with perfect matched DNA1 (CGA<sub>8</sub>GC) in PNA<sub>2</sub>:DNA (2:1) ratio for triplex formation. The stability of the triplexes containing the modification were examined by variable temperature UV absorbance. The formation of PNA:DNA complexes is indicated by sigmoidal transition with a maxima in derivative curve.<sup>[2,27]</sup> which represents the  $T_m$  for the complex. The results of  $T_m$  for various PNA<sub>2</sub>:DNA triplexes incorporating modified t\* at C and N termini and in the center are shown in Table 2. The modified t\* at N and C-termini stabilize the derived triplexes, while t\* at the center destabilizes the triplex, compared to the control unmodified *aeg*PNA (PNA1). The stabilization of PNA<sub>2</sub>:DNA triplex having N-terminal modification (PNA2) and C-terminal modification (PNA4) was 2.7 °C and 7.7 °C respectively over  $T_m$  of unmodified PNA1:DNA1 triplex (Table 2). PNA3:DNA1 triplex with t\* in the center was destabilized by 13.1 °C. The sequence specificity of PNA binding was investigated by measuring thermal stabilities of triplexes with DNA2 having a single mismatch base C in the middle shown in red (CGA<sub>4</sub>CA<sub>3</sub>GC). The  $T_m$ s of mismatch triplex PNA1 (control) and PNA2 were lowered by 10.6 °C and 10.8 °C respectively, while triplexes PNA3 and PNA4 with modifications in center and C-terminus did not bind to mismatch DNA2 (Table 2). These results suggest incorporation of *dap*PNA monomer in *aeg*PNA sequence can discriminate between triplexes with perfect complementary and single-mismatch complementary DNA. These results with triplexes encouraged us to synthesize mixed purine-pyrimidine PNA sequences incorporating t\* and study duplex formation with complementary DNA.

### Thermal Stability of PNA:DNA Duplex

To check the thermal stability of PNA:DNA duplexes, a model sequence GTAGATCACT was chosen, which has been used in a number of publications to evaluate the thermal melting of modified PNA:DNA duplexes.<sup>[17–20]</sup> *dap*PNA monomer was incorporated at desired position in the synthesized mixed purine-pyrimidine *aeg*PNA control sequence PNA5 to obtain PNA6–8. The thermal stabilities of duplexes of PNA5–PNA8 with complementary DNA3 (AGTGATCTAC, antiparallel) and DNA4 (CATC-TAGTGA, parallel) were studied by temperature dependent UV absorbance experiments. The melting temperature ( $T_m$ s) for PNA:DNA duplexes extracted from the UV-melting curves are shown in Table 3.

Depending on the site of incorporation, all *dap*PNA (t\*) sequences PNA6–PNA8 show substantial enhancement of derived antiparallel PNA:DNA duplex stability ( $\Delta T_{m3} = +5.1$  to  $+13.4$  °C) compared to the unmodified control PNA5. Single incorporation at N-terminus (PNA 6) resulted in enhancement of  $T_m$  by 5.1 °C while in the middle (PNA 7), it stabilized the duplex by 12.9 °C. The incorporation of two units of *dap*PNA (PNA8) enhanced the stability even better ( $+13.4$  °C) in comparison to duplex of control unmodified *aeg*PNA (PNA5).

To scrutinize the role of electrostatic interactions, the effect of salt concentration on thermal stability of *dap*PNA:DNA complexes was studied. The results show marginal decrease of  $-0.7$  °C in  $T_m$  for unmodified *aeg*PNA sequence when the salt concentration was increased from 10 mM to 100 mM. However, a sharp decrease of upto  $-11.1$  °C in melting temperature was observed for modified *dap*PNAs (Figure S7, ESI) clearly suggesting the electrostatic role-play in the stability of PNA:DNA complexes.

Since *dap*PNA is chiral, comparative selectivity in binding of DNA in parallel/antiparallel orientation was studied with *dap*PNA duplexes with DNA4 that can form parallel duplexes with PNA5–PNA8. It is seen from Table 3 that *dap*PNAs can form parallel duplexes with DNA4 but stability is lower than that of antiparallel

Table 2. UV- $T_m$  (°C) Studies of PNA<sub>2</sub>:DNA triplexes with matched DNA1 and mismatched DNA2.

Entry	Homooligomers	DNA1	DNA2
		$T_{m2}$ ( $\Delta T_{m2}$ ) in °C	$T_{m2}$ ( $\Delta T_{m2}$ ) in °C
PNA 1	TTTTTTT-Lys	42.1 (0)	31.5 (-10.6)
PNA 2	t*TTTTTTT-Lys	44.8 (+2.7)	34.0 (-10.8)
PNA 3	TTTt*TTT-Lys	29.0 (-13.1)	ND
PNA 4	TTTTTTTt*-Lys	49.8 (+7.7)	ND

Conditions: PNA strand concentration 1  $\mu$ M, 10 mM sodium phosphate buffer, pH 7.4, 10 mM NaCl. T: *aeg*PNA, t\*: *dap*PNA, DNA 1 = CGA<sub>8</sub>GC, DNA 2 = CGA<sub>4</sub>CA<sub>3</sub>GC, ND = No detectable binding

**Table 3.** UV- $T_m$  (°C) Studies of PNA:DNA duplexes with antiparallel DNA3 and parallel DNA4.

Entry	Mixed oligomers	DNA3	DNA4
		$T_{m3}$ ( $\Delta T_{m3}$ ) in °C	$T_{m4}$ ( $\Delta T_{m4}$ ) in °C
PNA 5	GTAGATCACT-Lys	44.7 (0)	38.1 (-6.6)
PNA 6	Gt*AGATCACT-Lys	49.8 (+5.1)	41.5 (-8.3)
PNA 7	GTAGAt*CACT-Lys	57.6 (+12.9)	48.4 (-9.2)
PNA 8	Gt*AGAt*CACT-Ly	58.1 (+13.4)	45.3 (-12.8)
	<sup>[a]</sup> GTAGAT <sup>R</sup> CACT-Lys	ND	---

Conditions: PNA strand concentration 1  $\mu$ M, 10 mM sodium phosphate buffer, pH 7.4, 10 mM NaCl. T: *aeg*PNA, t\*: *dap*PNA, DNA 3 = AGTGATCTAC, DNA 4 = CATCTAGTGA, ND = No detectable binding.

[a] cpPNA sequence from literature with *trans*(*R,R*)-stereochemistry.<sup>[19b]</sup>

duplexes by  $-8.3^\circ\text{C}$  to  $-12.8^\circ\text{C}$ . This shows distinctly better orientation selectivity of all the modified PNAs (PNA6–PNA8) binding to antiparallel DNA3 in comparison to parallel DNA4.

To investigate if the higher thermal stability seen for *dap*PNA complexes is sequence independent, another mixed purine-pyrimidine sequence PNA9 (control) and PNA10 that incorporates t\* at N-terminus and in the center were synthesized. Their duplex stability in antiparallel and parallel orientations with complementary DNA5 (ACTGAGGTAA) and DNA6 (AATGGAGTCA) were studied (Table 4). The UV-melting studies on modified PNA sequence (PNA10) incorporating two *dap*PNA units showed high thermal stability ( $\Delta T_{m5} = +6.3^\circ\text{C}$ ) for antiparallel DNA5 and better orientation selectivity against parallel DNA6 compared to unmodified *aeg*PNA control sequence PNA9 (Table 4). This confirmed the generality of stabilization of DNA duplexes by *dap*PNAs.

As discussed in the beginning, *dap*PNA structure can also lead to another backbone in which the chain runs in a different

direction involving secondary amine group to yield isomeric *secdap*PNA. Such isomeric PNA was synthesized (Figure 2C) using Fmoc chemistry in SPPS. Incorporation of *secdap*PNA monomer at desired positions of control *aeg*PNA<sub>8</sub> sequence (PNA1) gave PNA11–PNA13, which were evaluated for stability of *secdap*PNA:DNA complexes. The octameric *secdap*PNA poly T sequences (PNA11–PNA13) upon hybridization with DNA1, showed triplex formation, as evidenced by the UV Job's plot and CD spectra (Figure S9, S10 ESI). UV-melting studies on *secdap*PNA<sub>2</sub>:DNA triplexes showed that *secdap*PNA modification at N-terminal stabilizes triplex formation by  $3.5^\circ\text{C}$ , whereas middle and C-terminal modifications showed destabilizing effect (Table 5). The results were slightly better when compared to the analogous *pmg*PNA (Figure 1e) reported in literature where all modified triplexes were destabilizing. *pmg*PNA derived from proline is not cationic (at pH 7.0) in its backbone unlike *secdap*PNA which adds a cationic amino group to *pmg*PNA making *secdap*PNA triplex (PNA 11) thermally more stable. In case of mixed purine-

**Table 4.** UV- $T_m$  (°C) Studies of PNA:DNA duplexes with antiparallel DNA5 and parallel DNA6.

Entry	Mixed oligomers	DNA5	DNA6
		$T_{m5}$ ( $\Delta T_{m5}$ ) in °C	$T_{m6}$ ( $\Delta T_{m6}$ ) in °C
PNA 9	TIACCTCAGT-Lys	50.9 (0)	50.9 (0)
PNA 10	Tt*ACct*CAGT-Lys	57.2 (+6.3)	53.4 (-3.8)

Conditions: PNA strand concentration 1  $\mu$ M, 10 mM sodium phosphate buffer, pH 7.4, 10 mM NaCl. T: *aeg*PNA, t\*: *dap*PNA, DNA 5 = ACTGAGGTAA, DNA 6 = AATGGAGTCA

**Table 5.** UV- $T_m$  (°C) Studies of PNA<sub>2</sub>:DNA triplexes with matched DNA1 and mismatched DNA2.

Modification	Entry	Homooligomers	DNA1	DNA2
			$T_{m7}$ ( $\Delta T_{m7}$ ) in °C	$T_{m8}$ ( $\Delta T_{m8}$ ) in °C
<i>aegPNA</i>	PNA 1	TTTTTTTT-Lys	42.1 (0)	31.5 (-10.6)
	PNA 11	<u>t</u> *TTTTTT-Lys	45.6 (+3.5)	34.1 (-10.5)
<i>secdapPNA</i>	PNA 12	TTT <u>t</u> *TTTT-Lys	25.1 (-17.0)	ND
	PNA 13	TTTTTT <u>t</u> *-Lys	34.3 (-7.8)	22.3 (-12.0)

Conditions: PNA strand concentration 1  $\mu$ M, 10 mM sodium phosphate buffer, pH 7.4, 10 mM NaCl. T: *aegPNA*, t\*: *secdapPNA*, DNA 1 = CGA<sub>3</sub>GC, DNA 2 = CGA<sub>4</sub>CA<sub>3</sub>GC, ND = No detectable binding

pyrimidine sequence, *secdapPNA*:DNA duplexes showed no detectable melting transition.

## Discussion

Electrostatic interactions and stereochemistry play an important role in thermal stability of PNA:DNA complexes.<sup>[4,23–25]</sup> Introduction of a cationic group like amine group in the neutral PNA, which undergoes protonation under physiological conditions, increases backbone electrostatic interaction of the cationic PNA with anionic DNA. This electrostatic interactions increase the thermal stability of PNA:DNA complexes. On the other hand, the presence of chirality in PNA provides orientation selectivity for antiparallel or parallel binding of PNA with chiral DNA. The stereochemistry at the chiral center/s is a contributing factor in PNA backbone pre-organization and one PNA stereomer may preferentially bind to DNA than the other stereomer.<sup>[7,17–20]</sup> We surmised that the thermal stability of weakly binding stereomeric PNA can be improved by electrostatic interactions by addition of a cationic group in the PNA backbone. Introduction of a cationic amino group in weakly binding *trans*-(*R,R*) cyclopentyl ring of *cpPNA* lead to (*R,R*)-*dapPNA* monomer (Figure 1). PNAs incorporating *dapPNA* (PNA7) bound to DNA with higher thermal stability (Table 3) compared to the same sequence with *cpPNA* at same site (GTAGAICTACT), which did not bind to DNA as reported in literature.<sup>[19b]</sup> All *dapPNA* incorporated sequences PNA6–PNA8 showed high thermal stability for PNA:DNA duplexes with maximum  $\Delta T_m$  of 12.9 °C (compared to unmodified), and better selectivity for antiparallel duplexes with +9.2 °C for a single *dapPNA* middle modification (PNA7). The electrostatic interactions can be disrupted by addition of salt and in presence of increasing amounts of NaCl (10 mM–100 mM), PNA7 duplex with DNA, showed a sharp decrease of  $T_m$  up to –11.1 °C. This pointed to the role of electrostatic interaction in *dapPNA* duplexation. However, electrostatic interactions are sequence independent and may lower sequence fidelity in binding. The considerable

lowering of stability of duplexes with mismatch, suggested retention of sequence selectivity in binding despite of the additional stability offered by electrostatic interactions.

Another structural/conformational effect influencing stability is the ring puckering of pyrrolidine ring in *dapPNA*, that is different from that of cyclopentyl ring in *cpPNA*. The five-membered rings interconvert between envelope and twist conformation and the distortion made by the out-of-plane atoms generates ring pseudorotation. In saturated alicyclic rings such as cyclopentane, pseudorotational barrier is negligible whereas in pyrrolidine it is 1.2 Kcal/mol.<sup>[28]</sup> This suggests imposition of rigidity in pyrrolidine ring of *dapPNA*, locking the conformation for DNA binding. Solution state NMR study of unmodified PNA:DNA complexes suggested the  $\beta$ -dihedral angle between C2–C3 to be 141°.<sup>[29]</sup> One of the intermediate **9** for the synthesis of (*1R,2R*) *dapPNA* monomer **13** showed *endo* ring-pucker for the pyrrolidine ring with  $\beta$  dihedral angle between C2–C3 to be 103° that is close to the required  $\beta$ -dihedral angle for PNA:DNA complex formation. The  $\beta$ -dihedral angle in (*1R,2R*) *cpPNA* as calculated by molecular dynamics is in the range of 70° to 90°.<sup>[19a]</sup> The puckering of pyrrolidine ring thus reorganizes the PNA backbone, to a favorable  $\beta$ -dihedral angle between C2–C3 and thereby enhance the thermal stability with DNA.

A special characteristic of monomer **13** is that it can give rise to another backbone *secdapPNA* that has a free primary amino group and can become cationic in physiological conditions. The role of electrostatic interactions on cationic *secdapPNA* was evaluated by UV-thermal melting of corresponding PNA complexes with DNA and compared with reported *pmgPNA* which lacks the amino group. The  $T_m$  data showed that cationic *secdapPNA* forms stronger PNA<sub>2</sub>:DNA triplexes compared to neutral *pmgPNA*, further reinstating the role of electrostatic interactions in PNA:DNA stability. However, the stability of *secdapPNA* duplex with DNA was generally lower than unmodified *aegPNA*. This might be due to an unfavorable ring pucker due to the amide nitrogen in *secdapPNA*, which becomes part of the ring.

## Conclusion

In this study we designed and synthesized for the first time a dual *dap*PNA monomer that give rise to two different backbones named *dap*PNA and *secdap*PNA. The design was based on our hypothesis that introduction of a cationic group in stereochemically unfavorable PNA backbone for duplex formation should enhance the thermal stability of its complexes with DNA. The results showed that both *dap*PNA and *secdap*PNA with unfavorable stereochemistry for binding significantly stabilize its complexes with DNA mainly due to electrostatic interactions. The enhanced stabilization of PNA:DNA complexes is also accompanied by greater discrimination of mismatched sequences and better orientation selectivity between parallel and antiparallel DNA sequences. This highlights the role of interplay between electrostatic interactions and stereochemistry and might be useful in designing future PNA analogues.

## Experimental Section

All starting materials and reagents available commercially were used without further purification. Other details are provided in the Supporting Information.

**(3R,4R)-1-benzyl-3,4-dihydropyrrolidine-2,5-dione (1).** L-tartaric acid (45.0 g, 0.3 mol) in xylene (200 ml) stirred at room temperature, benzyl amine (32.7 ml, 0.3 mol) was added and refluxed using a dean stark apparatus till the appropriate amount of water (10.8 ml, 0.6 mol) was collected during 7–8 hrs. After cooling, the resulting solid was filtered and washed with ethanol followed by acetone to obtain product 1 as a light yellow solid which was recrystallized from ethanol to get a white solid. This was used for next step without further purification. Yield (59.8 g, 90%);  $[\alpha]_{25}^D = +138$  (c 1.0, MeOH); M.P. = 196–198 °C;  $^1\text{H NMR}$  (200 MHz, DMSO- $d_6$ )  $\delta$  7.26–7.11 (m, 5H, Ph), 6.25–6.17 (m, 2H, 2 $\times$ OH), 4.53–4.37 (m, 2H, benzyl CH<sub>2</sub>), 4.32–4.24 (m, 2H, 2 $\times$ CH);  $^{13}\text{C NMR}$  {H}(50 MHz, DMSO- $d_6$ ):  $\delta$  174.8, 136.2, 128.8, 127.8, 74.8, 41.4; MS (EI)  $m/z$ : Calculated for C<sub>11</sub>H<sub>12</sub>NO<sub>4</sub> [M + H]<sup>+</sup> is 222.07, Found 222.04 [M + H]<sup>+</sup>, 244.15 [M + Na]<sup>+</sup>.

**(3S,4S)-1-benzylpyrrolidine-3,4-diol (2).** To an ice-cooled solution of 1 (11.0 g, 49.7 mmol) in THF (300 ml) under nitrogen, Lithium Aluminium Hydride (5.7 g, 149.1 mmol) was added and refluxed for 12 hrs after which reaction was quenched with aqueous sodium sulphate solution. The resulting mixture was filtered, and the salt obtained was taken in diethyl ether and stirred for 2–3 hrs and filtered. Extraction in diethyl ether was repeated four times. The combined filtrate was concentrated and the residue was purified by column chromatography to obtain compound 2 as a white solid. Yield: (7.0 g, 73%);  $[\alpha]_{25}^D = +34$  (c 1.0, MeOH); M.P. = 101–103 °C;  $^1\text{H NMR}$  (200 MHz, CDCl<sub>3</sub>):  $\delta$  7.32–7.22 (m, 5H, Ph), 4.15–3.95 (m, 4H, 2 $\times$  OH (2H) and 2 $\times$ CH (2H)), 3.67–3.47 (m, PhCH<sub>2</sub>-diastereotopic,  $^2J = 12.6$  Hz, 2H), 2.89 (dd,  $J = 5.8$  Hz, 10.1 Hz, 2H, –CH<sub>2</sub>), 2.41 (dd,  $J = 3.9$  Hz, 10.3 Hz, 2H, –CH<sub>2</sub>);  $^{13}\text{C NMR}$  {H}(50 MHz, CDCl<sub>3</sub>):  $\delta$  137.0, 129.3, 128.3, 127.4, 78.1, 60.3, 60.0; MS (EI)  $m/z$ : Calculated for C<sub>11</sub>H<sub>16</sub>NO<sub>2</sub> [M + H]<sup>+</sup> is 194.11, Found 194.13 [M + H]<sup>+</sup>.

**(3S,4S)-1-benzyl-4-(tert-butyldimethylsilyloxy)pyrrolidin-3-ol (3).** Into the cold solution of diol 2 (3.3 g, 17.1 mmol) in THF (50 ml) under nitrogen, was added NaH (0.49 g, 20.5 mmol) and the reaction mixture was stirred in an ice bath for 15 min followed by the addition of tert-butyldimethylsilyl chloride (2.58 g, 17.1 mmol). The reaction mixture was stirred at room temperature for 12 hrs. Reaction monitored on TLC, after the completion of reaction as observed by TLC, solvent was evaporated to dryness and the residue was

dissolved in water and extracted with ethyl acetate. The solvent was evaporated under reduced pressure and product was purified on column chromatographic as light reddish oil. Yield: (4.2 g, 80%);  $[\alpha]_{25}^D = +26$  (c 1.0, MeOH);  $^1\text{H NMR}$  (200 MHz, CDCl<sub>3</sub>):  $\delta$  7.34–7.27 (m, 5H, Ph), 4.18–4.08 (m, 1H, <C-OCH), 4.00–3.92 (m, 1H, –CH <C-OCH), 3.74–3.56 (m, PhCH<sub>2</sub> diastereoscopic,  $^2J = 2.3$  Hz, 2H), 3.21 (dd,  $J = 6.2$  Hz, 10.1 Hz, 1H, –CH-OTBS), 2.80–2.60 (m, 3H), 2.20 (dd,  $J = 4.6$  Hz, 10.0 Hz, 1H), 0.87 (s, 9H, TBS), 0.05 (d,  $J = 3.9$  Hz, 6H, TBS);  $^{13}\text{C NMR}$  {H}(50 MHz, CDCl<sub>3</sub>):  $\delta$  137.5, 128.9, 128.2, 127.2, 79.1, 78.4, 61.0, 60.4, 60.1, 25.7, 17.9, -5.0; MS (EI)  $m/z$ : Calculated for C<sub>17</sub>H<sub>30</sub>NO<sub>2</sub>Si [M + H]<sup>+</sup> is 308.20, Found 308.19 [M + H]<sup>+</sup>.

**(3S,4S)-1-benzyl-3-O-mesyl-4-(tert-butyldimethylsilyloxy)pyrrolidine (4).** To a stirred solution of 3 (4.5 g, 14.6 mmol) and triethylamine (8.3 ml, 58.6 mmol) in dry DCM (40 ml) at 0 °C under nitrogen, was added methanesulfonyl chloride (2.3 ml, 29.2 mmol) in dry DCM (10 ml) over a period of 15 min. The reaction mixture was stirred for another 20 min. at room temperature, diluted with DCM (20 ml), washed successively with water, brine and dried over sodium sulphate. The organic layer was concentrated and purified to get mesyl 4 as a colourless oil. Yield: (4.2 g, 75%);  $[\alpha]_{25}^D = +38$  (c 1.0, MeOH);  $^1\text{H NMR}$  (200 MHz, CDCl<sub>3</sub>):  $\delta$  7.37–7.25 (m, 5H, Ph), 4.89–4.80 (m, 1H, –CH–OMs), 4.41 (dt,  $J = 6.2$  Hz, 1H, –CH–OTBS), 3.75–3.51 (m, PhCH<sub>2</sub>-diastereoscopic,  $^2J = 14.0$  Hz, 2H) 3.10 (dd,  $J = 6.6$  Hz, 9.6 Hz, 1H), 3.00 (s, 3H, mesyl CH<sub>3</sub>), 2.95–2.80 (m, 2H), 2.32 (dd,  $J = 5.9$  Hz, 9.7 Hz, 1H), 0.88 (s, 9H, TBS), 0.07 (d,  $J = 5.7$  Hz, 6H, TBS);  $^{13}\text{C NMR}$  {H}(50 MHz, CDCl<sub>3</sub>):  $\delta$  137.7, 128.6, 128.2, 127.1, 86.7, 76.6, 60.1, 59.8, 57.6, 38.1, 25.6, 17.8, -5.0; MS (EI)  $m/z$ : Calculated for C<sub>18</sub>H<sub>32</sub>NO<sub>2</sub>SSi [M + H]<sup>+</sup> is 386.18, Found 385.73 [M + H]<sup>+</sup>, 407.69 [M + Na]<sup>+</sup>.

**(3R,4S)-3-azido-1-benzyl-4-(tert-butyldimethylsilyloxy)pyrrolidine (5).** A mixture of mesyl 4 (17.0 g, 44.2 mmol) and sodium azide (23.0 g, 353.8 mmol) in dry DMF (200 mL) under nitrogen was heated at 100–110 °C for 12 hrs. After completion of reaction the solvent was removed under reduced pressure. The residue dissolved in ethyl acetate and washed with water, brine, dried over sodium sulphate and purified by column chromatography to yield 5 as light yellow oil. Yield: (7.0 g, 48%);  $[\alpha]_{25}^D = +50$  (c 1.0, MeOH);  $^1\text{H NMR}$  (200 MHz, CDCl<sub>3</sub>):  $\delta$  7.30–7.15 (m, 5H, Ph), 4.33 (q,  $J = 6.2$  Hz, 1H, –CH–OTBS), 3.68–3.45 (m, 3H, CH–N<sub>3</sub> and –CH<sub>2</sub>–Ph), 3.05–2.88 (m, 2H, –CH<sub>2</sub>), 2.54–2.36 (m, 2H, –CH<sub>2</sub>), 0.86 (s, 9H, TBS), 0.35 (d,  $J = 7.2$  Hz, 6H, TBS);  $^{13}\text{C NMR}$  {H}(50 MHz, CDCl<sub>3</sub>):  $\delta$  138.3, 128.4, 128.2, 127.0, 72.8, 61.2, 60.3, 60.1, 56.3, 25.6, 18.0, -5.2; MS (EI)  $m/z$ : Calculated for C<sub>17</sub>H<sub>29</sub>N<sub>4</sub>O<sub>2</sub>Si [M + H]<sup>+</sup> is 333.21, Found 333.85 [M + H]<sup>+</sup>.

**(3S,4R)-4-azido-1-benzylpyrrolidin-3-ol (6).** A 1 M solution of tetrabutyl ammonium fluoride in THF (23 mL) was added to a solution of 5 (5.0 g, 15.1 mmol) in THF (50 mL) under nitrogen at 0 °C. The reaction mixture was stirred at room temperature for 2 hrs, solvent was removed and extracted with ethyl acetate. The combined organic layers washed with brine, dried over sodium sulphate and purified by column chromatography to afford 6 as a colourless oil. Yield: (2.8 g, 86%);  $[\alpha]_{25}^D = +66$  (c 1.0, MeOH);  $^1\text{H NMR}$  (200 MHz, CDCl<sub>3</sub>):  $\delta$  7.38–7.20 (m, 5H, Ph), 4.38–4.28 (m, 1H, –CH–OH), 3.94 (q,  $J = 6.1$  Hz, 1H, –CH–N<sub>3</sub>), 3.65 (s, 2H, –CH<sub>2</sub>–Ph), 2.96–2.84 (m, 2H, –CH<sub>2</sub>), 2.75–2.55 (m, 2H, –CH<sub>2</sub>), 2.39 (br s, 1H, –OH);  $^{13}\text{C NMR}$  {H}(50 MHz, CDCl<sub>3</sub>):  $\delta$  137.7, 128.7, 128.2, 127.2, 71.2, 62.0, 60.1, 59.9, 56.2; MS (EI)  $m/z$ : Calculated for C<sub>11</sub>H<sub>15</sub>N<sub>4</sub>O [M + H]<sup>+</sup> is 219.12, Found 219.11 [M + H]<sup>+</sup>.

**(3R,4S)-1-benzyl-3-Boc-amino-4-hydroxypyrrolidine (7).** Azido-alcohol 6 (2.3 g, 10.6 mmol) in ethyl acetate (15 ml) taken in a hydrogenation flask in which Boc-anhydride (2.8 g, 12.7 mmol) and Raney-Ni (1.0 g) was added. The reaction mixture was hydrogenated in a parr apparatus maintaining the pressure 40–45 psi for 3 hrs and monitored by TLC. When reaction mixture showed disappearance of starting azide on TLC, catalyst was filtered off and the solvent was evaporated under reduced pressure. The product was purified by

column chromatography to yield **7** as a white solid. Yield: (2.3 g, 74%);  $[\alpha]_{25}^D = +9$  (c 1.0, MeOH); M. P. = 79–81 °C;  $^1\text{H NMR}$  (200 MHz,  $\text{CDCl}_3$ ):  $\delta$  7.36–7.20 (m, 5H, Ph), 5.31 (br s, 1H, –NH), 4.30–4.17 (m, 1H, –CH–OH), 4.14–3.97 (m, 1H, –CH–NH), 3.59 (s, 2H, –CH<sub>2</sub>–Ph), 3.05 (br s, 1H, –OH), 2.86–2.67 (m, 2H, –CH<sub>2</sub>), 2.65–2.45 (m, 2H, –CH<sub>2</sub>), 1.42 (s, 9H, *t*-Boc);  $^{13}\text{C NMR}$   $\{H\}$ (50 MHz,  $\text{CDCl}_3$ ):  $\delta$  155.8, 137.7, 128.8, 128.1, 127.0, 79.2, 69.8, 60.7, 60.0, 58.0, 52.1, 28.2; MS (EI) *m/z*: Calculated for  $\text{C}_{16}\text{H}_{25}\text{N}_2\text{O}_3$   $[M+H]^+$  is 293.18, found 293.75  $[M+H]^+$ , 316.19  $[M+Na]^+$ .

**(3S,4R)-1-benzyl-4-Boc-amino-3-O-mesylypyrrolidine (8)**. To a stirred solution of **7** (2.3 g, 7.9 mmol) and triethylamine (4.4 mL, 31.6 mmol) in dry DCM (20 mL) at 0 °C under nitrogen, was added methanesulfonyl chloride (1.2 mL, 15.8 mmol) in dry DCM (5 mL) over a period of 15 min and stirred for half an hour at 0 °C. The reaction mixture was diluted by adding 20 mL of DCM and washed successively with water, brine and dried over sodium sulphate. The organic layer was concentrated and purified to get mesylate **8** as a white crystalline solid. Yield: (2.4 g, 83%);  $[\alpha]_{25}^D = +37$  (c 1.0,  $\text{CHCl}_3$ ); M. P. = 130–132 °C;  $^1\text{H NMR}$  (200 MHz,  $\text{CDCl}_3$ ):  $\delta$  7.40–7.20 (m, 5H, Ph), 5.10–4.87 (m, 2H, –NH and –CH–OMs), 4.50–4.27 (m, 1H, –CH–NH), 3.65 (s, 2H, –CH<sub>2</sub>–Ph), 3.01 (s, 3H, mesyl CH<sub>3</sub>), 2.97–2.80 (m, 2H, –CH<sub>2</sub>), 2.49 (dd,  $J=7.5$  Hz,  $J=9.2$  Hz, 2H, –CH<sub>2</sub>), 1.44 (s, 9H, *t*-Boc);  $^{13}\text{C NMR}$   $\{H\}$ (MHz,  $\text{CDCl}_3$ ):  $\delta$  155.3, 137.5, 128.6, 128.3, 127.2, 79.8, 79.0, 59.6, 58.8, 56.5, 51.2, 37.7, 28.2; MS (EI) *m/z*: Calculated for  $\text{C}_{17}\text{H}_{27}\text{N}_2\text{O}_5\text{S}$   $[M+H]^+$  is 371.16, Found 372.09  $[M+H]^+$ , 394.13  $[M+Na]^+$ .

**(3S,4R)-4-azido-1-benzyl-3-Boc-aminopyrrolidine (9)**. To a stirred solution of mesyl **8** (2.5 g, 6.7 mmol) in dry DMF (30 mL) was added sodium azide (3.5 g, 53.8 mmol) at room temperature under nitrogen. The reaction mixture was heated at 60–70 °C for 18 hrs. The solvent was removed under reduced pressure and the residue was dissolved in water and extracted with ethyl acetate three times. The combined organic layer was washed with water, brine and dried over sodium sulphate and purified by column chromatography to afford azide **9** as a white solid. Yield (1.85 g, 86%);  $[\alpha]_{25}^D = -12$  (c 1.0, MeOH); M. P. = 70–72 °C;  $^1\text{H NMR}$  (200 MHz,  $\text{CDCl}_3$ ):  $\delta$  7.40–7.20 (m, 5H, Ph), 5.10–4.75 (m, 1H, –NH), 4.15–3.90 (m, 1H, –CH–NH), 3.85–3.70 (m, 1H, –CH–N<sub>3</sub>), 3.60 (s, 2H, –CH<sub>2</sub>–Ph), 3.04 (dd,  $J=6.8$  Hz,  $J=10.2$  Hz, 1H), 2.84 (dd,  $J=6.6$  Hz,  $J=9.8$  Hz, 1H), 2.54–2.32 (m, 2H, –CH<sub>2</sub>), 1.45 (s, 9H, *t*-Boc);  $^{13}\text{C NMR}$   $\{H\}$ (50 MHz,  $\text{CDCl}_3$ ):  $\delta$  154.9, 137.7, 128.6, 128.2, 127.2, 79.7, 66.6, 59.4, 58.0, 57.8, 56.5, 28.2; MS (EI) *m/z*: Calculated for  $\text{C}_{16}\text{H}_{24}\text{N}_5\text{O}_2$   $[M+H]^+$  is 318.19, Found 318.90  $[M+H]^+$ , 340.93  $[M+Na]^+$ .

**N-[(3R,4R)-1-benzyl-4-Boc-aminopyrrolidin-3-yl]-glycine ethyl ester (10)**. To solution of azide **9** (3.3 g, 10.4 mmol), in ethanol (20 mL), was added Raney-Ni (1.4 g) and the mixture was hydrogenated in a parr apparatus at 45 psi for about 3 hrs. After completion of reaction, the solvent was filtered over a celite pad and concentrated over rota evaporator to get colourless oil. The oil was taken in dry acetonitrile (50 mL), to which  $\text{K}_2\text{CO}_3$  (2.5 g, 18.1 mmol) was added and the mixture was stirred under nitrogen at 0 °C for 15 min followed by the addition of ethyl bromoacetate (1.4 mL, 12.5 mmol). The mixture was further stirred at room temperature for about 12 hrs. The solvent was evaporated, the residue was taken in ethyl acetate and washed with water, brine, dried over sodium sulphate and purified to get the compound **10** as a light yellow oil. Yield: (2.8 g, 71%);  $[\alpha]_{25}^D = +8.3$  (c 1.2,  $\text{CHCl}_3$ );  $^1\text{H NMR}$  (200 MHz,  $\text{CDCl}_3$ ):  $\delta$  7.38–7.15 (m, 5H, Ph), 5.13–4.93 (m, 1H, –NH(Boc)), 4.17 (q,  $J=7.1$  Hz, 2H, –CO<sub>2</sub>CH<sub>2</sub>), 3.93–3.72 (m, 1H, –NH), 3.59 (s, 2H, –CH<sub>2</sub>–Ph), 3.49 (s, 2H, –CH<sub>2</sub>–NH), 3.22–3.00 (m, 2H, 2×CH), 2.83–2.68 (m, 1H), 2.64–2.48 (m, 1H), 2.20–2.05 (m, 2H, –CH<sub>2</sub>), 1.43 (s, 9H, *t*-Boc), 1.26 (t,  $J=7.1$  Hz, 3H, –CO<sub>2</sub>CH<sub>2</sub>CH<sub>3</sub>);  $^{13}\text{C NMR}$   $\{H\}$ (50 MHz,  $\text{CDCl}_3$ ):  $\delta$  172.3, 155.2, 137.9, 128.7, 128.2, 127.1, 79.2, 65.2, 60.6, 59.9, 59.7, 58.7, 56.1, 48.9, 28.2, 14.1; MS (EI) *m/z*: Calculated for  $\text{C}_{20}\text{H}_{32}\text{N}_3\text{O}_4$   $[M+H]^+$  is 378.23, Found 377.13  $[M+H]^+$ , 399.02  $[M+Na]^+$ .

**N-[(3R,4R)-1-benzyl-4-Boc-aminopyrrolidin-3-yl]-N-(chloroacetyl)-glycine ethyl ester (11)**. To an ice-cooled stirred solution of **10** (2.55 g, 6.8 mmol) in dry DCM (30 mL) was added triethylamine (3.8 mL, 27.3 mmol). The reaction mixture was stirred for 15 min followed by the addition of chloroacetyl chloride (1.1 mL, 13.8 mmol) and continued to stir for another 10 hrs. The reaction mixture was diluted with 100 mL of DCM and washed with water, brine and dried over sodium sulphate and concentrated to obtain chloro compound **11** as a colourless liquid which was used without further purification. Yield: (2.6 g, 85%);  $^1\text{H NMR}$  (200 MHz,  $\text{CDCl}_3$ ):  $\delta$  7.38–7.18 (m, 5H, Ph), 5.23 (br s, 1H, –NH(Boc)), 4.51–4.05 (m, 6H, –CO<sub>2</sub>CH<sub>2</sub>, –CH<sub>2</sub>–CO<sub>2</sub>Et, 2×CH ring (2H)), 4.03–3.90 (m, 2H, –CH<sub>2</sub>Cl), 3.71–3.38 (m, 2H, –CH<sub>2</sub>–Ph), 2.91–2.57 (m, 2H, –CH<sub>2</sub>), 2.52–2.17 (m, 2H, –CH<sub>2</sub>), 1.43 (s, 9H, *t*-Boc), 1.24 (t,  $J=7.1$  Hz, 3H, –CH<sub>3</sub>). MS (EI) *m/z*: Calculated for  $\text{C}_{22}\text{H}_{33}\text{ClN}_3\text{O}_5$   $[M+H]^+$  is 454.21, Found 454.41  $[M+H]^+$ , 476.39  $[M+Na]^+$ .

**N-[(3R,4R)-1-benzyl-4-Boc-aminopyrrolidin-3-yl]-N-(thymine-1-acetyl)-glycine ethyl ester (12)**. To a solution of **11** (0.7 g, 1.5 mmol) in 10 mL dry DMF was added potassium carbonate (0.258 g, 1.9 mmol) followed by thymine (0.236 g, 1.9 mmol) at room temperature. The reaction mixture was stirred for 18 hrs at room temperature after which it was diluted with 100 mL of ethyl acetate and washed with water, brine and dried over sodium sulphate. The crude product purified by column chromatography to afford pure compound **12** as white solid. Yield: (550 mg, 85%);  $[\alpha]_{25}^D = -12$  (c 1.0, DMSO);  $^1\text{H NMR}$  (200 MHz,  $\text{CDCl}_3$ ):  $\delta$  7.38–7.15 (m, 5H, Ph), 7.10–6.95 (m, 1H, Thymine –NH), 4.90–3.93 (m, 8H, 2×CH (2H), ester –CH<sub>2</sub>, –CH<sub>2</sub>–CO<sub>2</sub>Et, –CH<sub>2</sub>–Thymine), 3.70–3.40 (m, 2H, –CH<sub>2</sub>–Ph), 3.35–3.10 (m, 1H), 2.90–2.55 (m, 2H, 2×CH), 2.45–2.15 (m, 2H, 2×CH), 1.90 (d,  $J=8.5$  Hz, 3H, Thymine CH<sub>3</sub>), 1.41 (d,  $J=9.5$  Hz, 9H, *t*-Boc), 1.30–1.15 (m, 3H, –CO<sub>2</sub>CH<sub>2</sub>CH<sub>3</sub>);  $^{13}\text{C NMR}$   $\{H\}$ (50 MHz,  $\text{CDCl}_3$ ):  $\delta$  169.7, 169.3, 167.7, 166.8, 164.4, 155.6, 151.3, 141.1, 137.9, 128.5, 128.3, 127.3, 127.2, 110.6, 62.1, 62.0, 61.2, 60.9, 60.3, 59.5, 56.6, 55.0, 47.5, 45.0; MS (EI) *m/z*: Calculated for  $\text{C}_{27}\text{H}_{38}\text{N}_5\text{O}_7$   $[M+H]^+$  is 544.27, Found 544.59  $[M+H]^+$ , 566.57  $[M+Na]^+$ .

**N-[(3R,4R)-1-Fmoc-4-Boc-aminopyrrolidin-3-yl]-N-(thymine-1-acetyl)-glycine (13)**. To an ice cooled solution of compound **12** (150 mg, 0.28 mmol) in 5 mL of ethanol was added 1.5 mL of 1 N sodium hydroxide solution in water and the reaction mixture was stirred in cold condition for 30 min. Water (10 mL) was added to the reaction mixture and solvent was removed on rotary evaporator to half of its volume. The remaining mixture was neutralized with Dowex H<sup>+</sup> resin to pH 6 and concentrated to get 130 mg of corresponding acid as white solid. This was taken in 10 mL of ethanol: water (8:2), added 10% Pd–C (65 mg, 50% by wt.) and was hydrogenated at 60 psi for 18 hrs. The reaction mixture thus obtained was filtered on celite pad and was concentrated to get 100 mg of crude amine. The crude amine was dissolved in 10 mL of acetone: water (2:1), cooled in an ice bath and sodium bicarbonate (24 mg, 0.28 mmol) was added followed by the addition of Fmoc-chloride (94 mg, 0.36 mmol). The reaction mixture was stirred at room temperature for 12 hrs after which the acetone was removed and the water layer was neutralized with saturated solution of potassium hydrogen sulphate and extracted with ethyl acetate three times. The combined ethyl acetate layers washed with water, brine and dried over sodium sulphate and purified by column chromatography to obtain monomer **13** as white solid. Yield: (100 mg, 57%);  $[\alpha]_{25}^D = -9$  (c 1.0, DMSO);  $^1\text{H NMR}$  (200 MHz,  $\text{CDCl}_3$ ):  $\delta$  10.26 (br s, 1H, –COOH), 7.80–7.15 (m, 8H, fmoc), 7.10–6.85 (m, 1H, Thymine –NH), 4.60–3.98 (m, 6H, –CH<sub>2</sub> & –CH fmoc, –CH ring, –CH<sub>2</sub>–CO<sub>2</sub>H), 3.95–3.55 (m, 3H, –CH<sub>2</sub>–Thymine, –CH ring), 3.45–3.10 (m, 2H, 2×CH), 2.40 (t,  $J=8.6$  Hz, 1H, –CH), 2.10–1.90 (m, 1H, –CH), 1.71 (s, 3H, Thymine –CH<sub>3</sub>), 1.39 (s, 9H, *t*-Boc);  $^{13}\text{C NMR}$   $\{H\}$ (50 MHz,  $\text{CDCl}_3$ ):  $\delta$  175.6, 143.7, 141.1, 127.8, 127.7, 127.1, 125.1, 125.0, 119.9, 49.5, 47.0, 30.6, 29.6, 28.2, 17.5; MS (EI) *m/z*: Calculated for  $\text{C}_{33}\text{H}_{37}\text{N}_5\text{O}_9$   $[M+Na]^+$  is 670.24, Found 671.92  $[M+Na]^+$ .

**Circular dichroism:** CD spectra were recorded on a Jasco J-715 spectropolarimeter. The CD spectra of the PNA:DNA complexes and the relevant single strands were recorded in 10 mM sodium phosphate buffer (pH 7.4) with appropriate NaCl concentration at 10 °C. The CD spectra of the oligothymine T8 single strands and mixed sequence PNAs and their complexes with DNA were recorded with accumulation of 5 scans from 300 to 195 nm using a 1 cm cell, a resolution of 0.1 nm, band-width of 1.0 nm, sensitivity of 2 mdegrees, response 2 sec and a scan speed of 50 nm/min. The PNA:DNA complexes were constituted by mixing appropriate strands in a 2:1 stoichiometry for triplexes and 1:1 stoichiometry for duplexes in buffer followed by heating to 90 °C for 5 mins and annealed by slow cooling to 4 °C.

**UV Job's Plot:** To a solution of DNA in 10 mM sodium phosphate at pH 7.4, were added portions of the complementary PNA oligomer to make 10 different fractions with mole ratio from 0–100% with fixed concentration. Then UV of each sample was scanned at temperature of 10 °C and the absorbance at 260 nm was recorded. This was plotted as a function of the mole fraction of PNA.

**UV- $T_m$  measurements:** UV melting experiments were performed on Cary 300 Bio UV-Visible Spectrophotometer equipped with a thermal melt system. The sample for  $T_m$  measurement was prepared by mixing calculated amount of stock oligonucleotide and PNA solutions together in 1 mL of 10 mM sodium phosphate buffer (pH 7.4). The samples 1 mL were transferred to quartz cell, sealed with Teflon stopper after degassing with nitrogen gas for 15 min and equilibrated at the starting temperature for at least 30 min. The optical density at 260 nm was recorded in steps from 10–85 °C with temperature increment of 0.5 °C/min. Nitrogen gas was purged through the cuvette chamber below 20 °C to prevent the condensation of moisture on the cuvette walls. Each melting experiment was repeated at least thrice. The results were normalized and analysis of data was performed using Microcal Origin (Microsoft Corp.). The absorbance or the percent hyperchromicity at 260 nm was plotted as a function of the temperature. The  $T_m$  was determined from the peaks in the first derivative plots and is accurate to  $\pm 1$  °C.

**Supporting Information** (see footnote on the first page of this article): Electronic Supporting Information (ESI) includes additional UV- $T_m$  curves, CD spectras and spectroscopic investigation such as LC–MS, NMR, IR, HPLC and MALDI-TOF for the synthesized compounds and PNA oligos.

## Acknowledgements

This work was supported by the Indian Institute of Science Education and Research (IISER) Tirupati and Department of Biotechnology (DBT grant BT/PR23487/NNT/28/1295/2017), Govt of India. The work was initiated at National Chemical Laboratory (NCL), Pune, India.

## Conflicts of interest

There are no conflicts to declare.

**Keywords:** aegPNA · Antisense oligonucleotides · Peptide nucleic acid · Stereochemistry

- [1] P. E. Nielsen, *Ann. Rev. Biophys. Biomol. Struct.* **1995**, *24*, 167–183.
- [2] B. Hyrup, P. E. Nielsen, *Bioorg. Med. Chem.* **1996**, *4*, 5–23.
- [3] L. Good, P. E. Nielsen, *Antisense Nucleic Acid Drug Dev.* **1997**, *137*, 431–437.
- [4] M. Egholm, O. Buchardt, L. Christensen, C. Behrens, S. M. Freier, D. A. Driver, R. H. Berg, S. K. Kim, B. Norden, P. E. Nielsen, *Nature* **1993**, *365*, 566–568.
- [5] K. Kilsa Hensen, H. Orum, P. E. Nielsen, B. Norden, *Biochemistry* **1997**, *36*, 5072–5077.
- [6] E. Uhlmann, A. Peyman, G. Breipohl, D. W. Will, *Angew. Chem. Int. Ed.* **1998**, *37*, 2796–2823; *Angew. Chem.* **1998**, *110*, 2954–2983.
- [7] a) K. N. Ganesh, V. A. Kumar, *Acc. Chem. Res.* **2005**, *38*, 404–412; b) K. N. Ganesh, V. A. Kumar, *Curr. Top. Med. Chem.* **2007**, *7*, 715–726.
- [8] P. E. Nielsen, *Acc. Chem. Res.* **1999**, *32*, 624–630.
- [9] P. E. Nielsen, *Mol. Biotechnol.* **2004**, *26*, 233–248.
- [10] R. Mitra, K. N. Ganesh, *Chem. Commun.* **2011**, *47*, 1198–1200.
- [11] R. Mitra, K. N. Ganesh, *J. Org. Chem.* **2012**, *77*, 5696–5704.
- [12] D. R. Jain, A. V. Libi M Lahiri, K. N. Ganesh, *J. Org. Chem.* **2014**, *79*, 9567–9577.
- [13] S. Ellipilli, S. Palvai, K. N. Ganesh, *J. Org. Chem.* **2016**, *81*, 6364–6373.
- [14] S. Ellipilli, K. N. Ganesh, *J. Org. Chem.* **2015**, *80*, 9185–9191.
- [15] P. Zhou, M. Wang, L. Du, G. W. Fisher, A. Waggoner, D. H. Ly, *J. Am. Chem. Soc.* **2003**, *125*, 6878–6879.
- [16] K. N. Ganesh, P. E. Nielsen, *Curr. Org. Chem.* **2005**, *4*, 931–943.
- [17] P. Lagriffoule, P. Wittung, M. Eriksson, K. K. Jensen, B. Nordkn, O. Buchardt, P. E. Nielsen, *Chem. Eur. J.* **1997**, *3*, 912–919.
- [18] T. Govindaraju, V. A. Kumar, K. N. Ganesh, *J. Am. Chem. Soc.* **2005**, *127*, 4144–4145.
- [19] a) M. C. Myers, M. A. Witschi, N. V. Larionova, J. M. Franck, R. D. Haynes, T. Hara, A. Grajkowski, D. H. Appella, *Org. Lett.* **2003**, *5*, 2695–2698; b) J. K. Pokorski, M. A. Witschi, B. L. Purnell, D. H. Appella, *J. Am. Chem. Soc.* **2004**, *126*, 15067–15073; c) H. Zheng, M. Saha, D. H. Appella, *Org. Lett.* **2018**, *20*, 7637–7640.
- [20] T. Govindaraju, V. A. Kumar, K. N. Ganesh, *J. Org. Chem.* **2004**, *69*, 5725–5734.
- [21] A. Slaitas, E. Yeheskiely, *Eur. J. Org. Chem.* **2002**, *14*, 2391–2399.
- [22] P. S. Lonkar, V. A. Kumar, *J. Org. Chem.* **2005**, *70*, 6956–6959.
- [23] T. Vilaivan, *Acc. Chem. Res.* **2015**, *48*, 1645–1656.
- [24] S. Sforza, G. Haaima, R. Marchelli, P. E. Nielsen, *Eur. J. Org. Chem.* **1999**, *197*–204.
- [25] N. T. S. De Costa, J. M. Heemstra, *PLoS One.* **2013**, *8*, 2–9.
- [26] A. M. D. A. Rocha Gonsalves, M. E. S. Serra, D. Murtinho, V. F. Silva, A. M. Beja, J. A. Paixao, M. R. Silva, L. A. Da Veiga, *J. Mol. Catal. A* **2003**, *195*, 1–9.
- [27] K. N. Ganesh, V. A. Kumar, K. A. Baravkar, *Supramolecular Control of Structure and Reactivity* (Eds.: A. D. Hamilton, Chapter 6) **1996**, 263.
- [28] L. Carballeira, I. Perez-Juste, *J. Chem. Soc. Perkin Trans. 2* **1998**, 1339–1345.
- [29] M. Eriksson, P. E. Nielsen, *Nat. Struct. Biol.* **1996**, *3*, 410–413.

Manuscript received: December 4, 2020

Revised manuscript received: January 11, 2021

Accepted manuscript online: January 11, 2021